International Information and Engineering Technology Association
Advancing the World of Information and Engineering

Spatial Regularity in the Distribution of Bed-Rock Mineralization (Based on the Example of a Section of the Vetreny Poyas Ridge, Russia)

Igor Movchan[1]*, Aleksandra Yakovleva[2], Zilya Sadykova[3], Darya Sekerina[1], Aleksander Kuzovenkov[4]

[1] Department of Geophysics, St. Petersburg Mining University, St. Petersburg 199106, Russia
[2] Department of Higher Mathematics, St. Petersburg Mining University, St. Petersburg 199106, Russia
[3] Department of Geophysics, Geoscan Ltd., St. Petersburg 194021, Russia
[4] Administration, SZGGK Geocomplex LLC, St. Petersburg 195265, Russia

Corresponding Author Email: igorb_movchan@mail.ru

ABSTRACT

This study aimed to identify characteristic properties of bedrock mineralization in the Vetreny Poyas Ridge, Russia, and develop an automated model to forecast gold-sulfide and gold-sulfide-quartz ore deposits based on geophysical and geochemical data integration. The research employed a combination of remote sensing, digital terrain modeling (DTM), geophysical potential fields, and discriminant analysis. Machine learning algorithms were applied to detect patterns in geodynamic zones, structural formations, and mineral occurrences. The chain fraction method was utilized for analytical continuation to enhance the predictive model's resolution. The findings confirmed that gold-sulfide mineralization correlates with discordant intersections of geodynamic zones and structural features. The predictive model successfully localized several high-potential mineral zones in the central and southeastern parts of the study area. Geochemical testing verified these findings, with significant gold anomalies aligning with predicted zones. The study demonstrates the potential of integrating AI-driven models with geophysical and geochemical data for enhanced mineral exploration. This method improves the accuracy of predicting mineralized zones in complex geological environments and can be adapted for use in other regions.

1. INTRODUCTION

In recent years, the exploration and prediction of bed-rock mineralization have emerged as pivotal challenges in the field of economic geology, underpinning the quest for sustainable and efficient resource extraction [1]. Traditional geophysical and geochemical exploration methods, though widely used, often fall short of accurately forecasting the spatial distribution of ore anomalies. Many existing studies have employed classical methods such as remote sensing and geological mapping, but the predictive power of these techniques is limited by the inability to fully integrate complex geological, geochemical, and geophysical data in a cohesive manner.

This challenge is particularly pronounced in regions with complex geological environments, such as the Vetreny Poyas Ridge, which was selected as the focus of this study. The ridge's intricate structural formations, shaped by a dynamic tectonic history, present a formidable test for traditional exploration techniques. This region, characterized by significant faulting, magmatism, and deformation, requires a more advanced approach to accurately predict mineralization patterns. However, accurately predicting the location of these deposits remains a challenge due to the region's heterogeneous and discontinuous tectonic features. By addressing the limitations of conventional methods, this study introduces an innovative approach that integrates AI-driven models and advanced geophysical data processing to more precisely map these complex mineral systems [2]. Tectonically, the experimental test site considered in this work is confined to the suture zone of the Belomorsky and Karelian geological blocks of the crystalline basement. With such a tectonic position, the leading geostructural elements of the studied territory are the East Karelian geodynamic zone formed in the Lower Proterozoic era by a family of inherited and age-varying rift-related synforms and the Sumozero-Kenozero greenstone complex of the Upper Archean era, represented by separate trough formations. In the conditions of deep discontinuous tectonic deposits and the background of regional granitization, here, in the range of 3.2-2.4 billion years, there have been several stages of basaltic-ultrabasic magmatism [3] associated with the possible gold ore specialization of the territory of the Vetreny Poyas ridge and its surroundings. In the geological section, one generally observes steeply falling contacts of structural and material complexes of different ages, overlapped by monoclinally overlying Cenozoic deposits. This complexity introduces significant uncertainty in the prediction of mineralization zones, as the spatial distribution of minerals is influenced by a myriad of interrelated geological factors that are difficult to quantify and model [4, 5]. While advances in remote sensing, data processing, and

computational modeling have provided new tools for mineral exploration, these technologies also come with limitations [6]. High-resolution data can be costly and time-consuming to acquire, and the computational demands of processing large datasets and running complex simulation models can exceed the available resources [6, 7].

Through this research, we contribute to the field by presenting an innovative solution to the multifaceted challenge of predicting bed-rock mineralization. Thus, the purpose of these studies was to determine the patterns in the system of a priori known bedrock occurrences and gold deposits previously identified in the vicinity of the experimental landfill, for extrapolation of gold-prospective areas within the boundaries of this test site based on the noted patterns. Within the framework of the stated goal, we solved the methodological problem of the systematic organization of the tested methods of qualitative and quantitative interpretation, as well as related concepts and physical analogies used in both geological exploration and engineering and geological projects [8-10].

Unlike previous efforts, which have largely approached these challenges in isolation, our methodology harmoniously integrates geophysical, geochemical, and environmental data through a cutting-edge computational platform. This platform not only streamlines the analysis of complex datasets but also introduces a novel, AI-driven approach to pattern recognition within geological data, significantly enhancing the accuracy of mineral localization predictions [11]. This research moves beyond isolated analyses of mineral occurrences by harmonizing diverse data sources through a computational platform designed to enhance the accuracy and efficiency of mineral localization. By employing machine learning algorithms to recognize patterns within geodynamic and structural data, this study offers a breakthrough in the automation of mineral exploration [11].

Following this introduction, this article unfolds in a structured manner, initially outlining the methodologies employed for integrating geophysical and geochemical data, followed by a detailed presentation of our findings and their implications for mineral exploration. Conclusively, we reflect on the significance of these insights within the broader context of geological research and propose directions for future studies, emphasizing our contributions to advancing mineral prediction techniques [12].

2. RESEARCH SIGNIFICANCE

The significance of this study lies in its innovative integration of geophysical and geochemical data through advanced computational models, markedly enhancing the precision of mineralization predictions. By addressing the spatial complexity and heterogeneity of geological formations with a novel, AI-driven approach, our research offers significant improvements over traditional mineral exploration methods.

3. MATERIALS AND METHODS

The initial matrices of potential fields were formed by referring to the planetary database of geophysical data publicly available at usgs.com and wdmam.org The detailing of several matrices was possible due to additional digitization of the 1:1,000,000 scale geophysical basis. Within the experimental test site, students conducted clarifying large-scale assessments of potential fields with equalization of multi-time and multi-scale data based on the methods used [13, 14] within the framework of an internship at the NWGGC Geocomplex LLC. The geological basis was formed based on the analysis of the works of the aforementioned authors, several published generalizations of the last twenty years, as well as the geological basis of scales 1:200,000 and 1:1,000,000 published in open access at vsegei.ru. A special emphasis is placed on the formation of the geological reference of the experimental test site in determining the position of gold ore bedrock occurrences and deposits, the clarification of which was facilitated by interaction with the management of NWGGC Geocomplex LLC. Considering the noticeably discretized digital models of geophysical fields, the generalized nature of the geological basis, and the remoteness of gold ore occurrences and deposits from the test site noted above.

According to the totality of joint interpretative assessments of a qualitative and quantitative nature, the accuracy of geostructural tracking on a remote basis in combination with DTM is up to the first meters, whereas for geophysical fields it is the first hundreds of meters [15].

As for the research methods, we note the need to use remote data analysis in combination with DTM at different scale levels at the first stage of interpretation [16-18]. This should involve processing the area outside the experimental test site to trace geostructural features correlated with a priori-specified gold ore reference samples. The next stage was to define parametric pattern recognition with training. The possibility of using regional digital models of Digital Orthophoto (DO) and Digital Terrain Model (DTM) in spatial connection with geophysical fields allowed us to refine the results of decoding potential and non-potential geofields by discriminant analysis [19].

3.1 Quantitative interpretation

Quantitative interpretation is a critical aspect of the study, aiming to translate complex geophysical data into actionable insights for mineral exploration. This process involved the calibration of multi-scale geophysical data with known geological formations, allowing for the extrapolation of mineralization zones. The data from remote sensing and digital terrain models (DTM) [20] were combined with geophysical potential fields to quantify the relationships between structural features and mineral occurrences. The method follows well-established geophysical principles for identifying potential zones of mineralization [7], which provide a basis for correlating geophysical anomalies with known geological structures.

3.2 Discriminant analysis

In this study, discriminant analysis was employed to differentiate between regions with and without mineralization potential, using geophysical and geochemical field data. Discriminant analysis, as described by Alahgholi et al. [15], is a statistical technique used to classify observations into distinct groups based on a set of predictor variables. For this research, it was applied to geophysical fields (such as gravity and magnetic anomalies) and geochemical markers, allowing us to draw clearer boundaries around areas of mineralization

potential. By training the model on known mineral deposits, we were able to predict the likelihood of gold ore occurrences in unexplored regions of the experimental test site. The discriminant function was derived using a training dataset of known gold occurrences, and a threshold probability of 0.35 was selected based on maximizing the accuracy of classification.

Like multi-scale decoding, discriminant analysis allows the extrapolation of prospective sites for gold mining to the limits of the experimental test site [17]. In addition to trained recognition, we utilized reference-free methods with established markers to detect mountain massif permeability zones. Comparing morpho-structural forecasts and reference-based recognitions, promising gold mining areas were identified, showcasing varied alignments with predictive markers [21-23].

Against the background of general descriptions of recalculations applied to commercial software, as well as scientific publications describing the analytical continuation in a general, operator form, we focused on three approaches: the Berezkin method, the Ermokhin chain fraction method, and GRAD technology. Among these three approaches, GRAD technology has been developed for the quantitative interpretation of the gravitational field. Our experience shows that it is also applicable for the recalculation of the magnetic field ΔT_a, but it gives a representative result (from the point of view of the geostructural image) only after reduction ΔT_a to the pole [24].

3.3 Chain fraction method

The chain fraction method was used for the analytical continuation of geophysical fields, which is essential for accurately predicting the depth and extent of subsurface structures. This technique, commonly utilized in geophysical exploration [25], involves breaking down complex geophysical signals into smaller, manageable segments (fractions), which can then be analyzed separately. By doing so, we were able to enhance the resolution of our predictive models, particularly in regions where the geology is highly discontinuous. The method was especially useful in refining the depth profiles of magnetic and gravitational fields, allowing for more precise tracking of ore-controlling structures [26].

4. RESULTS

Considering the previously noted metasomatic genesis of gold-sulfide and gold-sulfide-quartz ore occurrences, their attraction to the family of disjunctive breaks, which in our case have a relatively strict north-eastern extension, can be considered natural.

These disjunctive breaks surround the geodynamic zone of the north-western extension, to which intrusions of the basic and ultrabasic composition are confined [27, 28]. According to the tectonic scheme (Figure 1a), the geodynamic zone of the north-western extension refers to structures with shear kinematics, while sub-orthogonal disjunctive zones mark local stretching zones that control the areas of ore discharge.
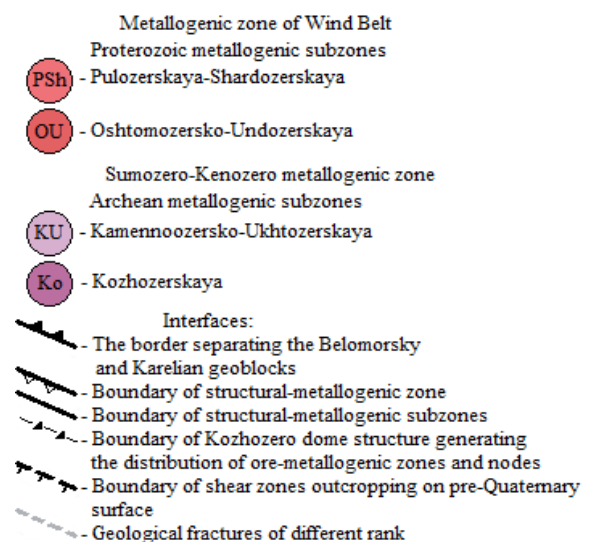
In the vicinity of a separate penetrative rock, these stretching zones form local quasi-periodic structures, and within each of them, the spatial increment between neighboring gold ore reference samples varies from 3 to 6km (Figure 1b). The quasi-periodic groups of gold ore reference samples are organized into quasi-periodic families, confined to the disjunctive areas of the sub-meridional and north-northwest extension, where the spatial increment is 60km or more. In addition to the recording of already known structural features, the operation of multi-level lineament decoding in Figure 2 illustrates the multi-scale parametric decoding of potential and non-potential geofields, emphasizing the spatial distribution of lineament structures and their correlation with regional geodynamic zones. At the small scale (1:2,500,000), the red contours outline the broad geophysical features, while medium-scale (1:500,000) adjustments enhance the resolution of localized disjunctive tectonic structures. The yellow contour at a detailed scale (1:50,000) highlights the experimental test site's geodynamic framework. These structural insights are crucial for identifying areas of increased permeability associated with potential mineralization. The mapping of ring structures happens in strict correlation to the areas of discordant intersection of geodynamic zones of different extensions, which allows for the marking of the area of increased permeability and associated local hydrothermal substitution with the designated ring structures [29].

(a) Tectonic scheme

LEGEND

Metallogenic zone of Wind Belt
Proterozoic metallogenic subzones

(PSh) - Pulozerskaya-Shardozerskaya

(OU) - Oshtomozersko-Undozerskaya

Sumozero-Kenozero metallogenic zone
Archean metallogenic subzones

(KU) - Kamennoozersko-Ukhtozerskaya

(Ko) - Kozhozerskaya

Interfaces:
- The border separating the Belomorsky and Karelian geoblocks
- Boundary of structural-metallogenic zone
- Boundary of structural-metallogenic subzones
- Boundary of Kozhozersky dome structure generating the distribution of ore-metallogenic zones and nodes
- Boundary of shear zones outcropping on pre-Quaternary surface
- Geological fractures of different rank

(b) Geological basis with the designation of ore reference samples

Figure 1. Primary extra-scale geological, structural, and tectonic basis in the vicinity of the experimental test site
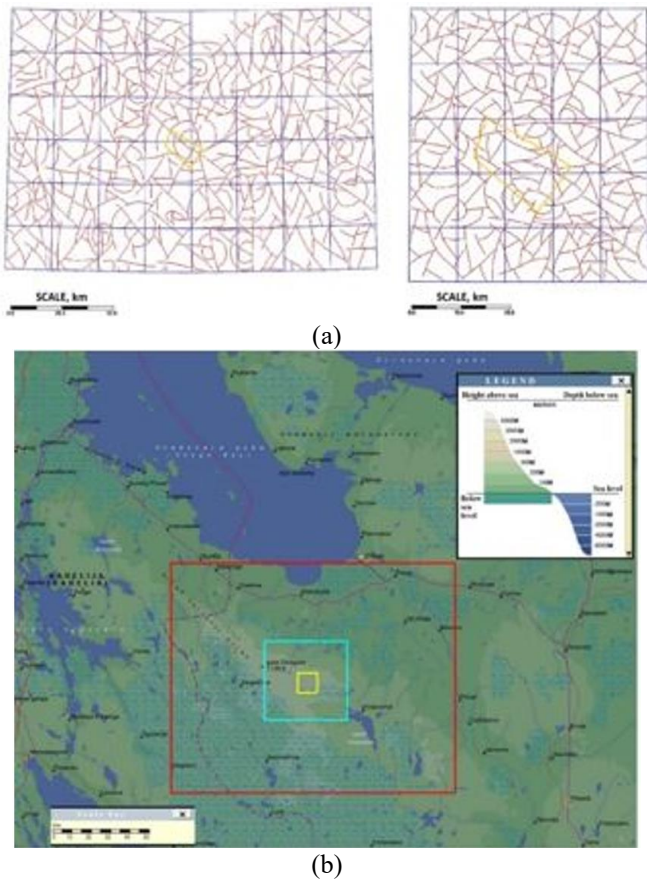
415

(a)

(b)

Figure 2. Multi-scale parametric decoding of potential and non-potential geofields for the studied territory, highlighting lineament structures and geodynamic features
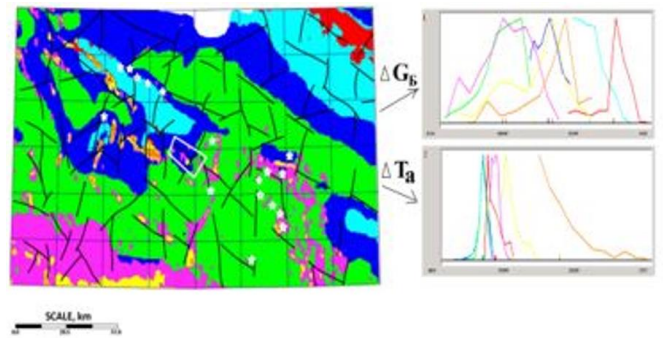
In the case of geoblock zoning, we used the calculation of the autocorrelation radius of geophysical potential fields in a sliding window, and the presence of obvious similarities in the final schemes allowed us to implement zoning according to a set of features based on the previously noted K-mean method (Figure 3). On the different-scale zoning schemes, two dominant stretches of the geostructural plan discussed earlier are manifested, namely, the north-western (shear), as well as the north-eastern (shear and separation), which surrounds it and is clearly subordinate to it. The sorted lineament structures from Figure 2 emphasize this feature, as well as the manifestation of the ring structure in Figure 3b, on the periphery of which the experimental test site is located.

Figure 3 presents geoblocking zoning results under varying scale conditions. At smaller scales (Figure 3a), the data highlight the attraction of gold ore reference samples to the boundaries of geoblock structures, with dominant structural stretches exhibiting a northwestern (shear) and northeastern (shear and separation) orientation. As the scale increases (Figure 3b), the local areas of high spatial variability become apparent, particularly near the experimental test site. These results are consistent with the deformation ellipsoid model (Figure 3c), which elucidates the spatial relationships between shear fractures and mineralized zones. Such multi-scale analyses are instrumental in identifying promising zones for mineral exploration.
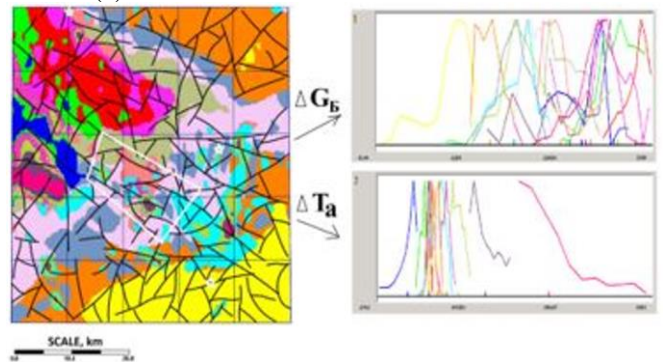
As for the position of gold ore reference samples when zoning on the smallest scale (Figure 3a), one can see the obvious attraction of these reference samples to the boundaries

of geoblock structures. When the scale is enlarged in Figure 3b, this pattern persists, but there is a clarification: near the boundaries of the experimental test site, gold ore objects are marked with areas with a large number of closely spaced areal structures, which marks local areas of increased spatial variability of geofields. Such sites should a priori mark objects promising for a certain grade of fossil mining [30, 31]. Similar sites are observed in the central part, on the south-western and north-western flanks of the experimental test site (Figure 3b). Against this background, the decryption scheme in Figure 3b captures the stretching of geodynamic zones, the morphology of which shows an amazing similarity with the model of the shear structure obtained based on the physical model of the deformation ellipsoid (Figure 3c).
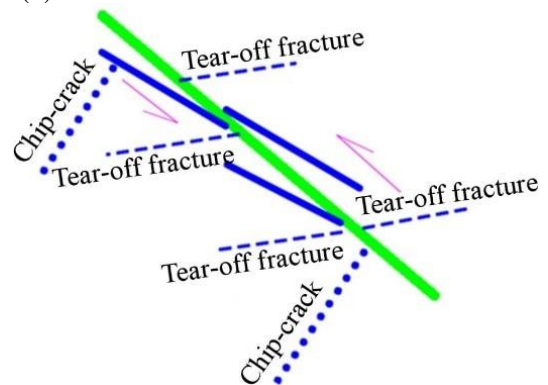
Turning to predictive schemes, we will again apply the variation of scales, as shown in Figure 2, and the results of morpho-structural schemes are shown in Figure 4.

(a) Under conditions of scale variation: small

Note: The experimental test site is marked with a white contour; endogenous ore reference samples are marked with white asterisks) and considering the deformation ellipsoid model.
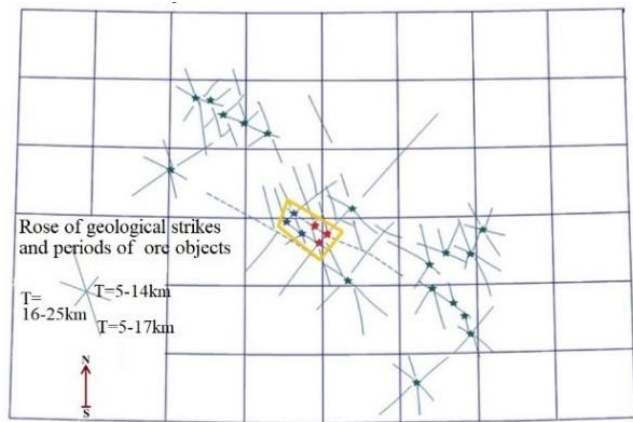
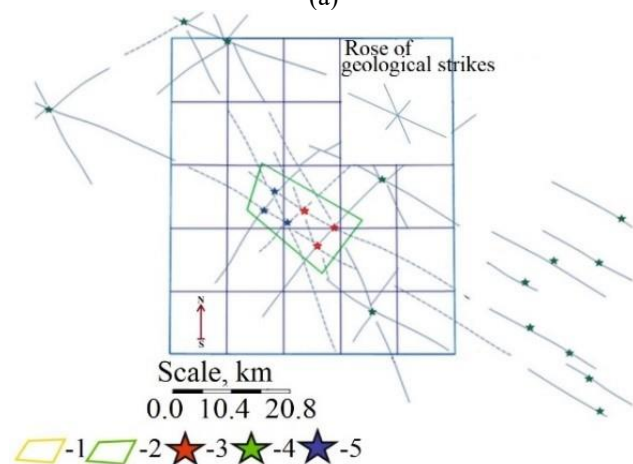(b) Under conditions of scale variation: medium

(c) Shear fractures and separation fractures in conditions of right-hand shift

Figure 3. The result of geoblocking zoning of the studied territory

(a)

Scale, km
0.0 10.4 20.8

☐ -1 ☐ -2 ★ -3 ★ -4 ★ -5

Note: Key features include quasi-periodic families of endogenous ore reference samples and discordant structures.

(b)

Figure 4. Morpho-structural analysis showing ore-controlling equidistant structures at varying scales

Figure 4 depicts the morpho-structural prognosis, employing the concept of ore-controlling equidistant structures. Quasi-periodic families of endogenous ore reference samples (Figure 4a) demonstrate spatial regularity within discordant zones. At medium scales (Figure 4b), extrapolation of these structures delineates areas with high mineralization potential, particularly along the southeastern flank of the experimental site. The observed ring structures further suggest localized hydrothermal activity, providing critical insights for prospecting mineral-rich zones.

The morpho-structural analysis presented in Figure 4 highlights the connection between discordant intersections of geodynamic zones and the predicted prospective geological bodies. These intersections control the spatial regularity of known gold ore occurrences. The predicted prospective areas were defined through the combination of small-scale (Figure 4a) and medium-scale (Figure 4b) analyses, where discordant zones marked by shear and separation structures correspond to areas with high mineralization potential [26].

Moreover, the structural mapping of lineaments, such as those depicted in Figure 4b, highlights areas of increased permeability and hydrothermal alteration. These areas are known to facilitate the concentration of mineral deposits, particularly in the vicinity of discordant zones. The connection between these structures and known gold mineralization is further supported by historical fieldwork, which has confirmed the presence of ore-bearing formations in similar tectonic settings [1, 8].

Considering the fact of spatial regularity manifested in the system of these GDZ, we extrapolate them according to the structure of the DTM and ΔT_a into the boundaries of the experimental test site. The predicted gold-prospective objects are located mainly on the south-eastern flank of the test site, which corresponds to the preliminary assessment obtained at the zoning stage. By increasing the scale (Figure 4b), we clarify the position of the objects prospective for gold mining, determining the area of priority confirmation in the northern part of the south-eastern flank of the test site, and the second confirmation stage in the southern part of the south-eastern flank and its central part. As can be seen from the comparison of Figure 4b with Figure 3b, the objects of the first and second stages of confirmation coincide with the areas of increased variability of the complex (geoblock) image of geofields [26].
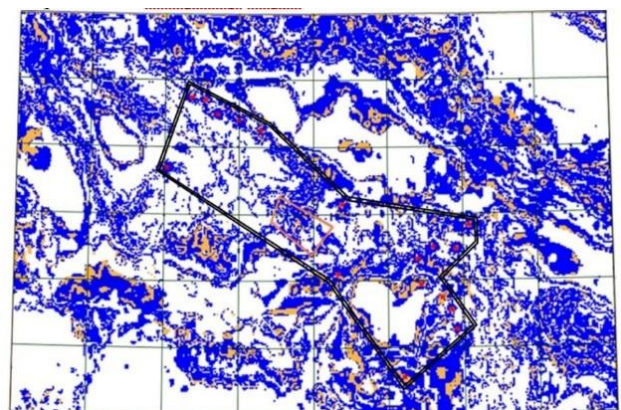
Scale, km
0.0 28.5 57.0

★ - reference ore objects
⬦ - contour of area of interpolation
▱ - investigated area
■ - 20% chance of ore finding
■ - 35% chance of ore finding

(a)
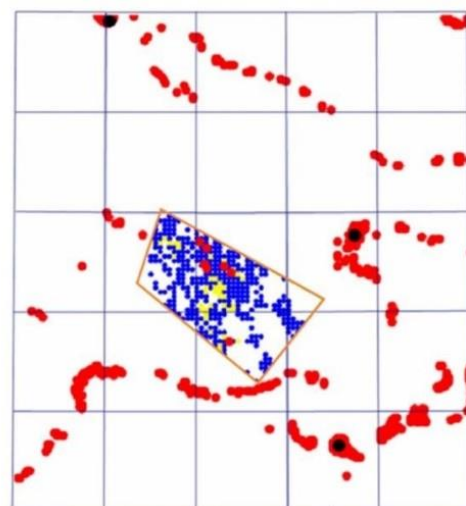
Scale, km
0.0 10.4 20.8

Legend
● reference ore objects
■ - 20% chance of ore finding
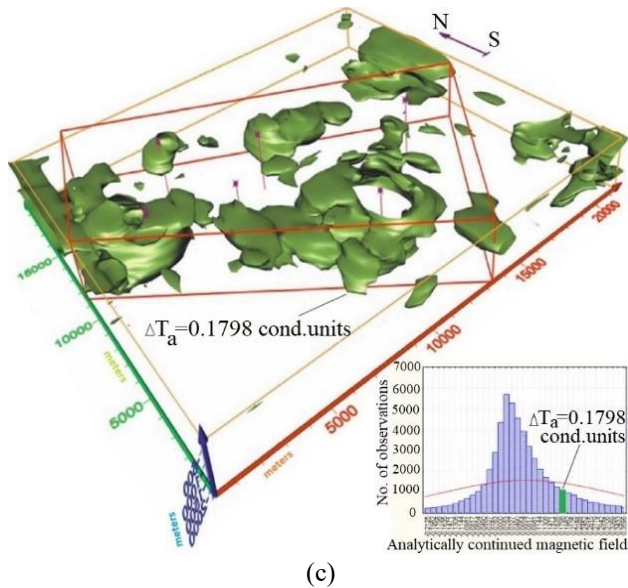■ - 35% chance of ore finding
■ - 45% chance of ore finding

(b)

$\Delta T_a = 0.1798$ cond.units

(c)

Figure 5. Results of pattern recognition for geophysical fields at different scales, showing forecast halos and prospective mineralization zones with 3D depth verification

Figure 5 summarizes the results of AI-driven pattern recognition applied to geophysical fields. At the regional scale (Figure 5a), forecast halos with probabilities ranging from 20% (blue) to 35% (orange) correspond to identified geodynamic zones. Medium-scale reconstructions (Figure 5b) refine these predictions, with red halos (45% probability) aligned with known mineralized zones. A three-dimensional depth-converted magnetic field model (Figure 5c) verifies the predicted prospective zones, marked in purple, within northwest-trending linear structures. The integrated approach demonstrates a robust capability for forecasting mineralization patterns in structurally complex areas.

Pattern recognition with training (Figure 5) has been performed, first of all, at the level of a regional survey for inclusion in the analysis of samples for all known reference objects of the central part of the Vetryanoy Poyas.
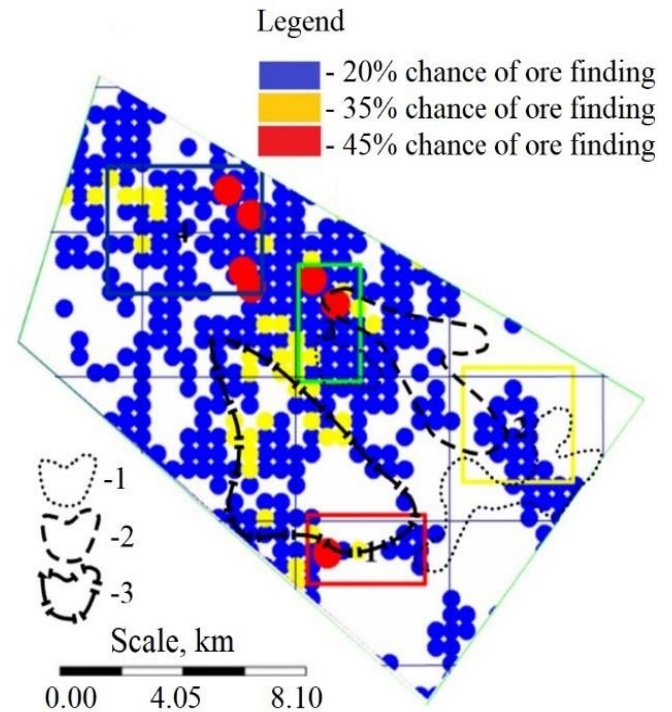
Figure 5a shows forecast halos derived from spectral channels of remote imaging, gravity, and magnetic fields, with probability levels assigned to prospective areas. The transformation results identify several prospective zones with different probabilities of detection, ranging from 20% to 45%. To support the correspondence between geophysical field transformation and prospective areas, additional geochemical verification was performed. As seen in (Figure 5b, the regions of higher probability (marked with red halos) correspond to areas of abnormal gold concentrations in secondary halos and placer samples collected from the study site. These areas also coincide with zones where the transformation of magnetic fields reveals deep-seated fault structures that are typically associated with mineralization [32].

Due to the significant spatial diversity of these reference objects, the statistical moments of the reference samples vary greatly in the area shown in Figure 5a, which, in particular, is indicated by the specifics of the geoblock reconstruction in Figure 3a. Nevertheless, the placement of the experimental test site between the ensembles of ore reference samples allows us to assert the representativeness of the forecast halos within its limits. At the level of medium-scale reconstruction (Figure 5b), we detail the primary forecast with an increased probability of detection: according to the ratio of regional

prognostic halos with a 35% or more probability of detection and medium-scale prognostic halos with a 45% or more probability of detecting a gold ore object, we highlight the southern part of the southeastern flank of the experimental site and its central part, which corresponds to the result of morpho-structural forecast.

5. DISCUSSION

The mineralization observed in the Vetreny Poyas Ridge is consistent with the broader geological context of the Fennoscandian Shield, which is renowned for its rich deposits of precious metals, including gold and nickel. The complex tectonic history of the Belomorsky and Karelian blocks has facilitated the formation of gold-sulfide and gold-sulfide-quartz mineralization, particularly in regions associated with rift-related synforms and disjunctive structures. The repeated phases of basite and ultrabasite magmatism during the Proterozoic and Archean eras created favorable conditions for ore deposition through hydrothermal processes. This research contributes to the understanding of these mineralization processes by validating the role of geodynamic zones as critical factors in ore formation [33].

Legend
- 20% chance of ore finding
- 35% chance of ore finding
- 45% chance of ore finding

Scale, km

0.00   4.05   8.10

Note: using data from NWGGC Geocomplex LLC): blue, red and yellow areas are the result of recognition with training (see Figure 5).
1: a complex geochemical anomaly;
2: an area of abnormal gold content in secondary scattering halos;
3: anomalous gold fields with detailed estimates in the basal horizon.
The numbers in rectangles are the recommended sequence of detailed ground confirmations.

Figure 6. Geochemical verification of parametric forecast results

As part of additional assessments of the structural control of the predicted gold ore development at the test site on a large scale, we are implementing a depth conversion by the ΔT_a chain fraction method. Algorithmically, the recalculation is carried out according to a system of profiles whose extension is sub-orthogonal to the dominant (north-western) extension of

the mapped geostructural plan [34-36]. The selection of isosurfaces is focused on visualizing the similarity of the geostructural plan, the elements of which would be spatially correlated with the position of most of the areas where gold occurrence was predicted. As can be observed from Figure 5, in the selected is surfaces of the deep image of the magnetic field, a largely segmented structure of mainly sub-latitudinal and northwestern extension is visualized, on the flanks of which five of the six selected objects prospective for gold mining are located. Special attention is paid to the objects located in the central part, as well as in the southern segment of the southeastern flank of the test site. Combining the results of all previous stages of qualitative interpretation allows us to speak about the principal prospects of the central part and the south-eastern flank of the test site, as we initially assumed, and now we have parametrically justified it (Figure 6).

These findings align with the work of Zhang et al. [4], who similarly employed a multi-scalar approach to identify prospective mineral zones in the Tongling Cu(-Au) District in China. Zhang et al. [4] also used a combination of geophysical and geochemical datasets to parametrize prospective mineralized zones, highlighting the significance of fault-related structures in guiding mineralization. In both studies, the use of remote sensing and AI-driven models was critical in refining the predictions, although the application of pattern recognition in the current study offers a more automated, scalable approach to mineral exploration.

Similarly, Lunkomo and Parfait [37] applied geostatistical methods in Iran's Bardaskan area to detect anomalous geochemical elements associated with mineralization.

In substantiation of the performed forecast, we used data from litho-geo-chemical tests, as well as further interpreted by us within the framework of the prognostic formulation of the problem described above [38]. These data are based on the analysis of the alluvial sediment placer samples in the channel part of surface multi-rank watercourses, implemented to map the features of gravitational separation and mechanical dispersion of gold and associated minerals [38-40]. Testing was carried out to a depth of no more than 1m with an increment varying within the first hundred meters. In addition, sampling on the outputs of pre-quaternary rocks with

inductively coupled plasma-atomic emission spectrometry (ICP-AES) quantitative analysis has been implemented [41-43]. According to the structure of the final scheme (Figure 6), we have the position of a complex gold halo combining placer samples with a gold content of more than $100mg/m^3$, litho-chemical samples of secondary scattering halos with a gold content of more than 100mg/t, as well as samples of bottom sediments with a gold content of 80 to 100mg/t, coinciding with the position of one of the promising objects, parametrically localized by us in the central part of the experimental test site (Table 1).

Additionally, Talapatra [43] in the work on concealed mineral deposits, highlighted the value of combining litho-chemical data with geophysical field data for predicting gold prospects. Their study demonstrated that areas with overlapping geophysical anomalies and high gold concentrations in secondary halos are prime targets for mineral exploration. Similarly, in our study, the presence of elevated gold content in secondary scattering halos and bottom sediments aligns with prospective objects previously identified by our geophysical models. However, the automated pattern recognition method employed here allows for a more efficient processing of large datasets, a significant improvement over the manual and semi-automated techniques used by Talapatra [43].

The second prospective object of the central part of the test site falls only in the area of abnormal gold content in the samples of secondary scattering halos (more than 100g/t). The prospective object situated in the southern part of the southeastern segment of the test site is located on the eastern flank of the complex halo and is characterized by a gold content in samples of secondary scattering halos up to 10mg/t. The prospective object of the northern part of the southeastern segment of the test site correlates with anomalous gold fields detected during detailed work in the basal horizon, as well as with the gold content in samples from secondary scattering halos up to 30mg/t. A prospective object in the northwestern segment of the experimental test site, manifested in the results of pattern recognition with training, but displayed in the family of other verification parameters in a mediocre manner; no geochemical confirmation.

Table 1. Indicators of the prospects of local sites of the experimental test site in Figure 6

Prospective Site No.	Characteristics of a Complex Geochemical Anomaly	Probability of Detection, According to Formal Recognition with Training	Geostructural Markers
1	- gold content in lithochemical samples of secondary scattering halos from 7 to 100mg/t; - gold content in the placer samples up to $50mg/m^3$; - the presence of abnormal gold fields in the basal horizon.	from 20% to 45%	- Gravitates to the zone of deep crust-mantle faults (according to gravimetric data).
2	- gold content in lithochemical samples of secondary scattering halos from 4 to 50mg/t; - the presence of abnormal gold fields in the basal horizon.	20%	- Located on the feathering fault of the north-eastern extension of the north-western extension shear structure (according to a priori geological and tectonic foundations).
3	- gold content in lithochemical samples of secondary scattering halos from 7 to 100mg/t; - the presence of abnormal gold fields in the basal horizon.	from 20% to 45%	- Gravitates to the area of intersection of deep crust-mantle faults of different extensions (according to gravimetric data).
4	- gold content in lithochemical samples of secondary scattering halos up to 10mg/t.	from 20% to 35%	- Placed on the edge seam of through-crust deformations (according to a priori geological and tectonic foundations).

This research demonstrates the effectiveness of the chain fraction method in enhancing the resolution of geophysical field data, enabling precise predictions about the depth and extent of mineralized zones. The success of the model in accurately predicting the spatial distribution of gold mineralization in the central and southeastern parts of the study site suggests that this approach could be scaled to other regions with similar tectonic settings [44].

6. CONCLUSIONS

This study successfully demonstrated the potential of combining geophysical, geochemical, and AI-driven techniques to predict mineralization zones in the Vetreny Poyas Ridge. By integrating remote sensing data, Digital Terrain Models, and geophysical field transformations, we identified several promising gold-sulfide and gold-sulfide-quartz mineralization zones, particularly in the central and southeastern parts of the experimental test site. The application of discriminant analysis and the chain fraction method allowed for accurate differentiation between mineralized and non-mineralized regions, while the use of AI pattern recognition streamlined the process, significantly improving the efficiency of mineral exploration efforts.

Prognostic schemes for endogenous mineralization give a representative predictive result in the context of the complex nature of assessments. In our case, the postulate of aggregation was expanded to include heterogeneous parametric estimates for the same geofields, as well as representative physical analogies and/or physical and geological models of a genetic or ore-controlling nature in the forecast.

In terms of the primary quantitative characteristics of geological and geophysical features, there is a chronic shortage of data during such surveys, which determined the structure of the formed multidimensional matrix of digital models of geofields, including DO, DTM, and two potential geophysical fields. The fact that at the first stage of quantitative interpretation, we identified prospective objects, most of which received further parametric and geochemical verification, shows that in the absence of geophysical fields, predictive schemes can also be made based on signs with less regulated access.

However, while the results are promising, there are several limitations to the current study that must be acknowledged. limitation lies in the reliance on AI-driven pattern recognition, which, while efficient, is constrained by the dataset on which it was trained. Further fieldwork and calibration are needed to ensure the model can adapt to new regions beyond the Vetreny Poyas Ridge, ensuring that predictions remain accurate in areas with different tectonic or mineralogical characteristics.

Also future research should aim to extend the AI-driven pattern recognition model to other geologically diverse regions to test its generalizability. By applying the model in regions with different geological settings-such as greenstone belts or volcanogenic massive sulfide deposits-researchers can evaluate its robustness and refine it to accommodate varying structural features.

REFERENCES

[1] Litvinenko, V.S., Petrov, E.I., Vasilevskaya, D.V., Yakovenko, A.V., Naumov, I.A., Ratnikov, M.A. (2023). Assessment of the role of the state in the management of mineral resources. Journal of Mining Institute, 259: 95-111. https://doi.org/10.31897/PML2022.100

[2] Irfan, U.R., Hasrianto, A.M., Imran, A., Maulana, A., Pachri, H. (2024). Integrative geophysical approach for enhanced iron ore detection: Optimizing geoelectrical and geomagnetic methods. International Journal of Design & Nature and Ecodynamics, 441-449. https://doi.org/10.18280/ijdne.190210

[3] Mezhelovskaya, S.V., Mezhelovskii, A.D., Bayanova, T.B. (2019). Mesoarchean granitoids of the Kozhozero block (Vetreny Poyas, southeast of Fennoscandia). In Materials of the XXVIII All-Russian Youth Conference "Structure of the Lithosphere and Geodynamics", pp. 104-105. https://www.crust.irk.ru/images/upload/newsfond296/1859.pdf#page=104.

[4] Zhang, Z., Wang, G., Ding, Y., Carranza, E.J.M. (2021). 3D mineral exploration targeting with multi-dimensional geoscience datasets, Tongling Cu (-Au) District, China. Journal of Geochemical Exploration, 221: 106702. https://doi.org/10.1016/j.gexplo.2020.106702

[5] Alzubaidi, L., Zhang, J., Humaidi, A.J., Al-Dujaili, A., Duan, Y., Al-Shamma, O., Santamaría, J., Fadhel, M.A., Al-Amidie, M., Farhan, L. (2021). Review of deep learning: Concepts, CNN architectures, challenges, applications, future directions. Journal of Big Data, 8: 1-74.

[6] Bykowa, E., Skachkova, M., Raguzin, I., Dyachkova, I., Boltov, M. (2022). Automation of negative infrastructural externalities assessment methods to determine the cost of land resources based on the development of a "thin client" model. Sustainability, 14(15): 9383. https://doi.org/10.3390/su14159383

[7] Kalinin, D.F., Yanovskaya Yu. A., Dolgal, A.S. (2021). Using statistical methods for interpreting potential fields to study the tectonic structure of prospective territories for oil and gas extraction. Geologiya Nefti I Gaza, 2: 27-36.

[8] Kalinin, D.F., Yanovskaya Yu. A., Dolgal, A.S. (2019). Results of the profile complex interpretation of geopotential fields by the method of empirical mode decomposition (EMD) in order to assess the prospects for oil and gas potential. Geofizika, 1: 2-12.

[9] Egorov, A.S., Prischepa, O.M., Nefedov, Y.V., Kontorovich, V.A., Vinokurov, I.Y. (2021). Deep structure, tectonics and petroleum potential of the western sector of the Russian Arctic. Journal of Marine Science and Engineering, 9(3): 258. https://doi.org/10.3390/jmse9030258

[10] Ding, X., Li, F., Li, H., Liu, B. (2020). Study on formation mechanism and evolution model of sliding surface of bedding mining slope. Journal of Mining and Safety Engineering, 152(5): 1019-1026.

[11] Koteleva, N.I., Kuznetsov, V.V., Vasilyeva, N.V. (2021). A simulator for educating the digital technologies skills in industry. Part One. Dynamic simulation of technological processes. Applied Sciences, 11: 10855. https://doi.org/10.3390/app112210885

[12] Skublov, S.G., Mikhaylov, A.A., Sokolov, A.A. (2023). Th-rich zircon from a pegmatite vein hosted in the Wiborg rapakivi granite massif. Geosciences, 13(12): 362-375. https://doi.org/10.3390/geosciences13120362

[13] Mingaleva, T.A., Shakuro, S.V., Egorov, A.S. (2023).

Study of the influence of factors determining the results of geophysical surveys in territories contaminated with light non-aqueous phase liquid. Russian Journal of Earth Sciences, 23(1): ES1002. https://doi.org/10.2205/2023ES000831

[14] Levashova, E.V., Popov, V.A., Levashov, D.S., Rumyantseva, N.A. (2022). Distribution of trace elements controlled by sector and growth zonings in zircon from a miaskite pegmatite of the Vishnegorsky massif, the Southern Urals. Journal of Mining Institute, 254: 136-148. https://doi.org/10.31897/PMI.2022.29

[15] Alahgholi, S., Shirazy, A., Shirazi, A. (2018). Geostatistical studies and anomalous elements detection, Bardaskan Area, Iran. Open Journal of Geology, 8(7): 697-710. https://doi.org/10.4236/ojg.2018.87041

[16] Alekseenko, V.A., Shvydkaya, N.V., Puzanov, A.V., Nastavkin, A.V. (2020). Landscape monitoring studies of the North Caucasian geochemical province. Journal of Mining Institute, 243: 371-378. https://doi.org/10.31897/PMI.2020.3.371

[17] Mvile, B.N., Abu, M., Kalimenze, J. (2021). Trace elements geochemistry of in situ regolith materials and their implication on gold mineralization and exploration targeting, Dodoma Region, East Africa. Mining, Metallurgy & Exploration, 38(5): 2075-2087. https://doi.org/10.1007/s42461-021-00450-7

[18] Glazunov, V.V., Ageev, A.S., Gorelik, G.D., Sarapulkina, T.V. (2021). Results of comprehensive geophysical studies on the search for crypts on the territory of suburban necropolis of Tauric Chersonese in the Karantinnaya Balka. Journal of Mining Institute, 247: 12-19. https://doi.org/10.31897/PMI.2021.1.2

[19] Bretar, F., Chehata, N. (2009). Generating digital terrain model: Joint use of airborne lidar data and optical images. Traitement Du Signal, 26(2): 145-159.

[20] Wang, Y., Zhao, H., Sheng, Y., Kang, N. (2015). Construction and application of 3D geological models for attribute-oriented information expression. Journal of Applied Science and Engineering, 18(4): 315-322. https://doi.org/10.6180/jase.2015.18.4.01

[21] Egorov, A.S., Bolshakova, N.V., Kalinin, D.F., Ageev, A.S. (2022). Deep structure, tectonics and geodynamics of the Sea of Okhotsk region and structures of its folded surroundings. Journal of Mining Institute, 257: 703-719. https://doi.org/10.31897/PMI.2022.63

[22] Fomin, S.I., Govorov, A.S. (2023). Validation of the chosen cutoff grade value in open pit mine design. Mining Informational and Analytical Bulletin, (12): 169-182.

[23] Bolshakova, N.V., Fedorova, K.S. (2021). The possibilities of using a qualitative interpretation of the potential for creating a zonal-block model of the northern flank of the okhotsk sea region. In Engineering and Mining Geophysics 2021. European Association of Geoscientists & Engineers, 2021(1): 1-7. https://doi.org/10.3997/2214-4609.202152157

[24] Hasach Albasri, N.A.R., Shakir, H.S., Al-Jawari, S.M. (2023). Monitoring and prediction functional change of land uses toward urban sustainability. International Journal of Sustainable Development and Planning, 18(7): 2015-2023. https://doi.org/10.18280/ijsdp.180703

[25] Movchan, I.B., Yakovleva, A.A. (2019). Wave analogies for generalized description of geodynamic zones. International Journal of Innovative Technology and Exploring Engineering, 8(6): 863-868.

[26] Li, H.L., Zhang, Z.Q., Yang, W. (2021). Stability analysis of slope based on limit equilibrium method and strength reduction method. Annales de Chimie-Science des Matériaux, 45(5): 379-384. https://doi.org/10.18280/acsm.450503

[27] Fernandes-Popova, A., Gulin, V.D., Senchina, N.P., Mingaleva, T.A. (2020). Estimation of the dependence of the quality of machine prediction of structural surfaces on potential fields on the completeness of the training sample. Intellektualnyi Analiz Dannykh V Neftegazovoi Otrasli, 2020: 23.

[28] Ren, Q., Meng, X. (2022). Study on mechanical response and stability algorithm of soft and hard rock interbedded slope excavation. Complexity, 2022(1): 3331097. https://doi.org/10.1155/2022/3331097

[29] Senchina, N., Grigoriev, G., Gulin, V. (2023). Combining non-seismic and seismic information for geological understanding-A case study. In E3S Web of Conferences. EDP Sciences, 376: 01067. https://doi.org/10.1051/e3sconf/202337601067

[30] Khokhlov, S., Abiev, Z., Makkoev, V. (2022). The choice of optical flame detectors for automatic explosion containment systems based on the results of explosion radiation analysis of methane-and dust-air mixtures. Applied Sciences, 12(3): 1515. https://doi.org/10.3390/app12031515

[31] Aizhong, L., Jia, X. (2020). Mechanical analytical method for dangerous sliding surface and stability safety factor of slope. Journal of Engineering Geology, 568: 1-7.

[32] Abdullahi, N.K., Ahmad, M.S., Abubakar, A. (2018). Application of electrical resistivity tomography technique for delineation of gold mineralization in Bugai town, Birnin Gwari, Kaduna, North Western Nigeria. Environmental and Earth Sciences Research Journal, 5(1): 29-35. https://doi.org/10.18280/eesrj.050105

[33] Odhipio, D.A., Tamelegu, J.Z., Mulekya, M.K., Kasekete, D.K., Kawa, G.N., Wazi, R.N. (2023). Geochemical assessment of mineral occurrences in the Karibumba region in the territory of Beni, Democratic Republic of the Congo. Environmental and Earth Sciences Research Journal, 10(2): 41-51. https://doi.org/10.18280/eesrj.100202

[34] Miller, A.A., Gorelik, G.D., Budanov, L.M. (2019). Substantiation of the optimal gis complex for the allocation of water-Containing reservoirs on the example of the analysis of well logging results in the leningrad region. In Engineering and Mining Geophysics 2019 15th Conference and Exhibition. European Association of Geoscientists & Engineers, 2019(1): 1-8. https://doi.org/10.3997/2214-4609.201901693

[35] Oganezov, A.V. (1997). Patent No. 2097794 RF. Method for determining the spatial coordinates of geological formations.

[36] Lai, T.W., Ji, Z.Y., Wu, H.G., Zhang, S.L., Lei, H., Liang, Y. (2021). Geological analysis and model test of bedding rock cutting landslide. Advances in Civil Engineering, 2021(1): 9948691. https://doi.org/10.1155/2021/9948691

[37] Lunkomo, S., Parfait, M.M. (2023). Geochemistry and structural inputs of the mineralized quartz veins from Imonga mining area, Maniema, DR Congo: General overview. Environmental and Earth Sciences Research

Journal, 10(1): 26-32. https://doi.org/10.18280/eesrj.100104

[38] Senchina, N.P., Asoskov, A.E., Gorelik, G.D. (2023). Evaluation of displacements caused by strike-slip deformations using correlation characteristics based on potential field data. Russian Journal of Earth Sciences, 23(4): 4013. https://doi.org/10.2205/2023ES000847

[39] Stern, R.J. (2023). The Orosirian (1800-2050Ma) plate tectonic episode: Key for reconstructing the Proterozoic tectonic record. Geoscience Frontiers, 14(3): 101553. https://doi.org/10.1016/j.gsf.2023.101553

[40] Duryagina, A.M., Talovina, I.V., Lieberwirth, H., Ilalova, R.K. (2022). Morphometric parameters of sulphide ores as a basis for selective ore dressing. Journal of Mining Institute, 256: 527-538. https://doi.org/10.31897/PMI.2022.76

[41] Smith, J.V. (2022). Potential for descending meteoric water recharge in hydrothermal systems as a pathway for carbon dioxide sequestration. GEOMATE Journal, 23(100): 78-85.

[42] Prischepa, O.M., Koval, V.V., Zakharchenko, M.V. (2023). Theoretical and methodological approaches to identifying deep accumulations of oil and gas in oil and gas basins of the Russian Federation. Frontiers in Earth Science, 11: 1-35. https://doi.org/10.3389/feart.2023.1192051

[43] Talapatra, A.K. (2020). Different types of geochemical explorations. In Geochemical Exploration and Modelling of Concealed Mineral Deposits. Springer, Cham, pp. 87-115. https://doi.org/10.1007/978-3-030-48756-0_4

[44] Pourgholam, M.M., Afzal, P., Yasrebi, A.B., Gholinejad, M., Wetherelt, A. (2021). Detection of geochemical anomalies using a fractal-wavelet model in Ipack area, Central Iran. Journal of Geochemical Exploration, 220: 106675. https://doi.org/10.1016/j.gexplo.2020.106675